



Texture Characterization of CT Images Based on Ridgelet Transform

V.R. Ratnaparkhe^{*}, R.R. Manthalkar⁺, Y.V. Joshi⁺

^{*}Government Polytechnic, Aurangabad,

⁺S.G.G.S. Institute of Engineering and Technology, Nanded*

[patwadkar.varsha, rmanthalkar, yashwant.joshi]@gmail.com

Abstract

Human vision system has limitations in distinguishing the broad range of gray level values. Human eye can discriminate pixel intensities up to 15-30 gray levels. This restricts the qualitative analysis of radiological images. Hence quantitative analysis is preferred to reveal more information from the image. This article presents texture feature based approach for biomedical image analysis. Images acquired from Computerized Tomography (CT) scan machine have been used for the work. A novel method of texture feature extraction based on Ridgelet transform has been reported in this paper. In the first step, work involves determination of texture features from Region of Interest (ROI). Energy and entropy in partitions of Ridgelet transform images represent texture features. During the next step of work, two-class and multi-class classification has been carried out. Percentage Correct Classification for Ridgelet based energy and entropy features and comparative analysis of performance measures for different organ images have been reported.

Keywords: Texture; Ridgelet Transform; Classification

1. Introduction

Texture can be defined as a set of local neighborhood properties of the gray levels of an image region. Texture analysis examines the small regular variations in intensity. It examines the relation of intensity of a point with respect to surrounding. Quantitatively, texture describes the two dimensional arrays of variations while the qualitative definition of texture is based on the fineness or coarseness of the image. Texture can be described by uniformity, density, coarseness, roughness, regularity, linearity, directionality, frequency and phase. Texture perception has many dimensions and the method of texture extraction depends on application.

Qualitative observations in image interpretation depend on the performance of first and second order visual tasks by radiologists. Human eye can identify the first order

visual data but its response to second order data is variable. Pixel intensities up to 15-30 gray shades can only be discriminated by eye. Hence quantitative evaluation can be achieved using computer based image analysis. Quantitative analyses allow additional digital manipulation of data to overcome some of the limitations of qualitative interpretation. For quantitative analysis, generally texture based analysis is preferred because it is important to extract maximum information from the medical images [1-5].

In medical imaging, texture is important, because it is difficult to classify human organ tissues using shape or gray level information. Position, shape and size of organ may vary for different patients. Size of organs may vary in different exposure slices of the same patient. Even by changing slice thickness, image information changes. Formation of image is based on absorption of X rays in tissue, which may depend on age of patient. Since, analysis based on these variable factors is difficult, texture based delineation is preferred.

Three principal approaches are used to describe the texture of a region viz. statistical, structural and spectral. Early approaches for texture analysis focused on the analysis of first order or second order statistics and stochastic models such as Gaussian Markov random fields and auto regression. First order statistical parameters consider the property of gray level and do not consider the spatial distribution. Second order statistics takes into account spatial distribution of gray levels, and examples includes Haralik transform, Unser's sum and difference histograms etc [6]. Recent developments in spatial/ spatial frequency analysis such as Gabor filters, wavelet transformation and wavelet frames provide good multi resolution analytical tools for texture analysis and classification [7,8,9,10,11].

Texture analysis has important role in computer vision and pattern recognition. It includes applications in industrial inspections, shape analysis, satellite imaging, medical diagnosis etc. In medical field texture plays vital role. Typical applications of medical imaging and analysis algorithms are Digital subtraction angiographies based on subtraction of images, study of heart walls and chambers based on boundary identification, location of tumors, detection of disease at early stage, delineation of organs, differential diagnosis, indexing and retrieval of organ images based on texture features extraction, ejection fraction computation using motion tracking, etc.

*This research was supported by AICTE grant 8022/RID/NPROJ/RPS-23/2003-04.



Literature survey reveals the use of texture in medical imaging. Some of the referred work has been included here.

McPherson used textural parameters to identify acute ischemia. An average of absolute differences of gray levels has been used, which shows variation after coronary occlusion. Haendehe reported the difference in skewness of gray level in healthy myocardium and necrosed myocardium [5]. Mammograms of breasts with increased fibro glandular density represent the skewed histograms giving negative values. Mammograms of fatty breasts give positive skewness. The skewness measure was found to be useful in predicting the risk of breast cancer [12]. Use of Haralik transforms for texture identification and use of Hopfield Neural Network to identify the similar features in the given CT or Magnetic Resonance Imaging (MRI) image has been reported [6]. The multi channel filtering has been reported for segmentation of echo cardio graphic images. The images are pre filtered by a bank of even symmetric Gabor filters. By applying the non-linear transform to the filtered images, texture signature is found out. Segmentation is done based on these [7]. Gabor based image representation is performed in [13]. Gabor based feature vector for texture is extracted. The target images of four types of hepatic tissues have been used. Retrieval of similar class has been identified based on measurement of Euclidean distance for a query image. In [14] authors have reported detection of malignancy in digital mammography images using texture analysis based on Chebyshev moments and log polar transformation.

2. Ridgelet Transform

Transform domain representation of a CT tissue image is important in characterization of texture. A representation of image data capturing the underlying intensity variations is essential to analyze the texture.

Wavelets provide a very sparse and efficient representation for piecewise smooth signals having finite singularities. But it cannot efficiently represent discontinuities along edges or curves in images or objects except in horizontal and vertical directions. To characterize texture in an efficient way a transform that captures singularities along lines and edges should give better representation. Ridgelet transform is a very good candidate for this. The good performance of wavelets in one-dimensional domain is lost when they are applied to images using two-dimensional (2D) separable basis since they are not able to efficiently code one-dimensional singularities. The Ridgelet transform achieves very compact representation of linear singularities in images [15]. To characterize texture in an efficient way the transform that captures singularities along lines and edges namely Ridgelet transform should give better representation.

Continuous Ridgelet transform (CRT) for a given image $I(x, y)$ is defined as:

$$CRT_f(u, v, \theta) = \int_{\mathbb{R}^2} \psi_{u,v,\theta}(x, y) I(x, y) dx dy \quad (1)$$

Where $\psi_{u,v,\theta}(x, y)$ in 2D are defined from a wavelet function in 1-D as

$$\psi_{u,v,\theta}(x, y) = \frac{1}{\sqrt{u}} \psi\left(\frac{x \cos \theta + y \sin \theta - v}{u}\right) \quad (2)$$

Separable continuous wavelet transform of $I(x, y)$ in \mathbb{R}^2 space is written as,

$$CWT_f(u_1, u_2, v_1, v_2) = \int_{\mathbb{R}^2} \psi_{u_1, u_2, v_1, v_2}(x, y) I(x, y) dx dy \quad (3)$$

Where

$$\psi_{u_1, u_2, v_1, v_2}(x, y) = \psi_{u_1, v_1}(x) \psi_{u_2, v_2}(y) \quad (4)$$

These 2D wavelet transforms [CWT] are similar to Ridgelet except the point parameter v_1 and v_2 are replaced by line parameter (v, θ) [15]. Thus wavelets are functions with scale and point position and Ridgelets are the functions with scale and line position. Hence wavelets are effective in representing point singularities. Ridgelets are effective in representing singularities along the line. Ridgelet can be considered as concatenation of one-dimensional (1D) wavelets along the line. Wavelet and Ridgelet transforms are related by Radon transform.

Radon Transform

The Radon transform is a projection of the image intensity along a radial line oriented at a specific angle. Radon transform extracts lines in edge-dominated images. Given an integrable bivariate function $I(x, y)$, its Radon transform (RDN) is defined by:

$$RDN_f(\theta, t) = \int_{\mathbb{R}^2} I(x, y) \delta(x \cos \theta + y \sin \theta - t) dx dy \quad (5)$$

The Continuous Ridgelet Transform (CRT) is simply the application of one-dimensional wavelet to the slices of Radon transform.

$$CRT(u, v, \theta) = \int_{\mathbb{R}} \psi_{u,v}(t) RDN_f(\theta, t) dt \quad (6)$$

$$CRT(u, v, \theta) = \int_{\mathbb{R}^2} \psi_{u,v,\theta}(x, y) I(x, y) dx dy \quad (7)$$

Here $\psi_{u,v}(t)$ is the wavelet function and $\psi_{u,v,\theta}$ is the Ridgelet function.

Ridgelet transform is the application of a 1 D wavelet transform to the slices of Radon transform. Candes and Donoho developed a system of representations named Ridgelet, which deal effectively with line singularities in 2-D. The idea suggested, is to map a line singularity into a point singularity using the Radon transform. Then, the wavelet transform can be used effectively to handle the point singularity in the Radon domain. However, finite Ridgelet transform is only suitable for images of prime-



pixels length. The good performance of wavelets in one-dimensional domain is lost when they are applied to images using 2D separable basis since they are not able to efficiently code one-dimensional singularities. The Ridgelet transform achieves very compact representation of linear singularities in images [15-16]. In order to apply Ridgelets to digital images a discrete transform is required, which needs the discrete Radon transform. In [15], Do and Vetterli propose a procedure that is invertible, orthogonal and achieves perfect reconstruction: the FiniteRidgelet Transform (FRIT). FRIT is based on the Finite Radon Transform (FRAT), which is defined as summations of image pixels over a certain set of lines.

For the finite Radon transform, image size is considered as prime number P . Various lines on this image are considered to find the Radon coefficients. The lines are obtained by varying slope. Two lines of different slopes intersect at one point. Consider $L_{k,l}$ denotes the set of points that make up a line on the lattice Z_p^2 . By taking discrete Wavelet transform of each FRAT projection, the discrete Ridgelet transform is obtained. The result is Finite Ridgelet Transform (FRIT). FRIT is defined by equation:

$$FRIT[k, m] = \left\langle FRAT_f[k, \cdot], \omega_m^{(k)}[\cdot] \right\rangle \quad (8)$$

$$FRIT[k, m] = \sum_{l \in Z_p} \omega_m^{(k)}[l] \langle f, \varphi_{k,l} \rangle \quad (9)$$

Here, $\varphi_{k,l}$ is the FRAT frame and $\omega_m^{(k)}$ is the basis function. Hence the FRIT frame is represented as:

$$\rho_{k,m} = \sum_{l \in Z_p} \omega_m^{(k)}[l] \varphi_{k,l} \quad (10)$$

This algorithm is insensitive to changes in gray levels [15,17-18].

FRIT transformed image is split into n partitions. Feature vector obtained based on this is represented as

$$F_s = [f_1, f_2, f_3, \dots, f_n] \quad (11)$$

The suffix indicates the dataset of specific organ. Suffix S, B, L and K indicate spleen, bladder, liver and kidney organ features respectively.

With reference to equation (10), each element in feature vector is obtained as

$$f_n = \frac{1}{i_{\max} j_{\max}} \sum_{i_n=1}^{i_{\max}} \sum_{j_n=1}^{j_{\max}} \left| \rho_{k+i_n, m+j_n} \right| \quad (12)$$

Here k and m indicate the start of partition. Similarly, entropy features based on Ridgelet transform have been worked out for the dataset of four organs. Similar analysis for each organ data set is carried out.

3. Classification

Classification can be of supervised and non-supervised types. Supervised learning is a process of designing a pattern classifier using a training set of patterns of known class. Non-supervised learning is to identify cluster or natural groups in the feature space [19,20,21]. A Classifier maps objects from the feature space into its output space after training. Classifiers are a special type of mapping, as their output spaces are related to class membership. In general a mapping converts data from one space to another. Using a training set a classifier can be trained such that it generalizes this set of examples of labeled objects into a classification rule. Such a classifier can be linear or nonlinear. The space defined by the actual set of features is called the feature space. Objects are represented as points or vectors in this space [22,23].

New objects in a feature space are usually gradually converted to labels by a series of mapping followed by a final classifier [22]. The effectiveness of features is generally assessed by classifier performance. The performance of classifiers gives different classification results for same features. A performance measure should be independent of classifier performance. Bayes classifier is included here as an example.

Bayes Classifier has decision function of the following form,

$$d_j(x) = p(x|w_j)p(w_j) \quad (13)$$

Where $j = 1, 2, 3 \dots w$

$p(x|w_j)$ is the probability density function of the pattern vectors of class of w_j . Considering the probability density function as Gaussian, $p(x|w_j)$ is expressed as,

$$p(x|w_j) = \frac{1}{2\pi^{n/2} |c_j|^{1/2}} \cdot \exp \left[\frac{-1}{2} \left[(x - m_j)^T c_j^{-1} (x - m_j) \right] \right] \quad (14)$$

c_j is covariance matrix of class w_j . m_j is mean vector of class w_j . Expressing it using Logarithm,

$$d_j(x) = \ln \left[p(x|w_j)p(w_j) \right] \quad (15)$$

$$d_j(x) = \ln p(x|w_j) + \ln p(w_j) \quad (16)$$

$$d_j(x) = \ln p(w_j) - \frac{n}{2} \ln 2\pi - \frac{1}{2} \ln |c_j| - \frac{1}{2} \left[(x - m_j)^T c_j^{-1} (x - m_j) \right] \quad (17)$$

The term $\frac{n}{2} \ln 2\pi$ is same for all the classes and therefore, it can be deleted and hence

$$d_j(x) = \ln p(w_j) - \frac{1}{2} \ln |c_j| - \frac{1}{2} \left[(x - m_j)^T c_j^{-1} (x - m_j) \right] \quad (18)$$

K-Nearest Neighbor Classifier, Linear Bayes Normal Density Classifier & Back-propagation trained feed-



forward neural net Classifier, Parzen Classifier etc. are different examples of classifiers [22].

Confusion matrix obtained during classification, gives numbers of true positive, true negative, false positive and false negative images. Based on this the accuracy, precision, sensitivity and specificity is computed. Specificity is a statistical measure to indicate how well the negative cases are handled. The specificity is related to true negatives of all the negative cases in the dataset. Specificity is defined by the formula

$$\text{Specificity} = \frac{\text{Number of true negatives}}{\text{Number of true negatives} + \text{number of false positives}}$$

Sensitivity indicates how well a given condition is correctly identified. Sensitivity is the proportion of true positive of all the positive classes in the dataset. It is defined by the formula

$$\text{Sensitivity} = \frac{\text{Number of true positives}}{\text{Number of true positives} + \text{Number of false negatives}}$$

Precision is obtained by dividing the number of true positives with the total true positives. Precision is a measure of exactness or fidelity. It is defined as the number of true positives divided by the total number of elements labeled to be belonging to the class. In general, 100% precision for a class means that every item, which is labeled as belonging to the class, really belongs to it. But precision does not comment on the item, which is misclassified to other class. It is the probability that a randomly selected item is relevant to the class. Accuracy is ratio of addition of true positives and true negatives to total number of organs.

4. Implementation

Figure 1 shows the Ridgelet based texture extraction method. The tissue images acquired from CT scan machine have been used for this work. Images of various CT scanning modes viz, abdominal CT scan, Lower abdomen and Pelvis CT scan etc, have been acquired. The actual region of interest (ROIs) of spleen, bladder, liver and kidney are cropped from images and stored in the form of database.

4.1 Ridgelet based features for normal organ images

All images of normal i.e. healthy organs have been considered here. ROI size is 13 X 13 or 31 X 31 depending on the size of organs. For this work, 124 liver images, 41 bladder images, 31 spleen images and 106 kidney images are used.

The second database of 54 liver images, 63 kidney images, 28 bladder images and 37 spleen images has been used. Only sample results of second database are represented in this paper. Figure 2 shows sample of Spleen and Figure 3 shows the ROI of Spleen. To compute the Ridgelet transform, first the Fourier transform of the ROI is calculated.

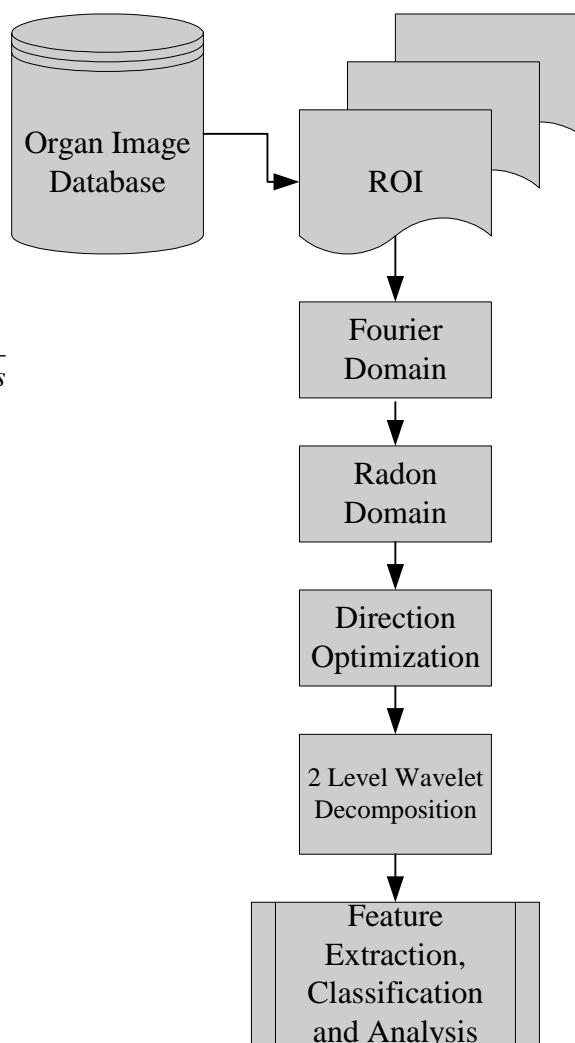


Figure 1: Methodology of Ridgelet Transform Based Analysis

When there is ridge in the image the spatial frequency representation will also show its dominance with some shift in the direction in Fourier domain [24,25]. Hence to explore the ridge like primitives, it is necessary to interpolate and convert the Fourier Transform to Polar form. The Radon Transform achieves this. The Radon Transform is computed only for optimum directions.



Figure 2: Sample image (Spleen)





Figure 3: ROI of sample Size 13 X 13

Optimum directions in Radon transform, develops the corresponding spatial frequency localization. 1D wavelet decomposition is applied to each column of Radon transform. This enhances the frequency localization in chosen directions. The result image of Ridgelet transform, applied on Figure 2 spleen, is indicated in Figure 4. Two levels of decomposition were implemented for this work.

Using PR Toolbox and linear discrimination classifier, performance of features has been analyzed. Two class, three class and four class classifier performances have been observed.

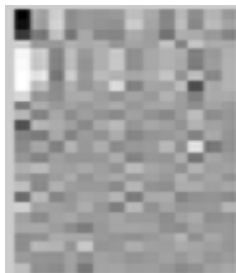


Figure 4: Finite Ridgelet Transform Image

The 66% data is considered as training set for the classifier. Sample scatter plots included in Figure 5 and Figure 6 indicate the discrimination of two classes in feature space. Figure 7 shows variations of texture features for different data sets based on energy and entropy texture features.

Table 1 shows the comparative results. It shows percentage Correct Classification (PCC) values for two and multi class classification. Classification results have been used to represent sensitivity, specificity, and precision and accuracy parameters to study the performance of Ridgelet based features.

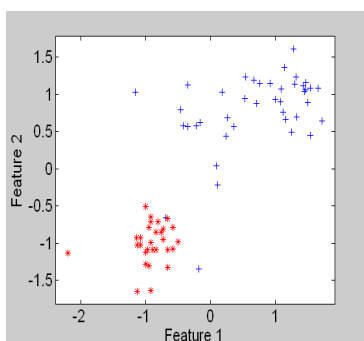


Figure 5: Scatter plot of Ridgelet Based Entropy Features Bladder Spleen Data

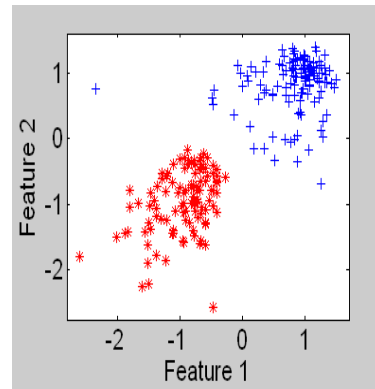


Figure 6: Scatter plot of Ridgelet Based Entropy Features Liver Kidney Data

Entropy is a statistical measure of randomness that can be used to characterize the texture of the input image. Entropy measures the information in the signal. It indicates uniformity [4-5,12,26]. It is given by equation

$$\text{Entropy} = -\sum (p_i \cdot \log(p_i)) \quad (19)$$

Where, p_i indicates the Ridgelet coefficient.

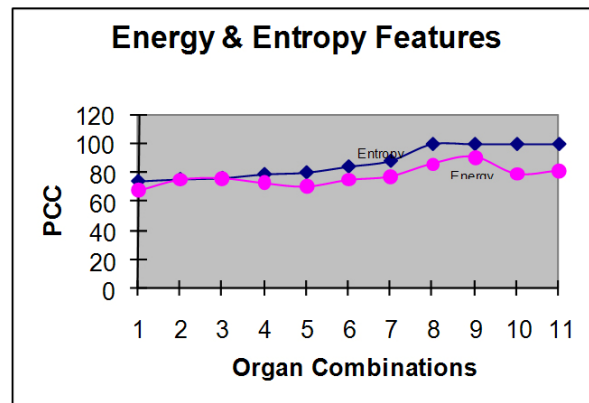


Figure 7: Comparison of Ridgelet Based Features

Table 1: Percentage Correct Classification (PCC) results		
Image Classes	PCC for Entropy	PCC for Energy
Liver & Kidney	100	86.41
Liver & Spleen	100	91.15
Kidney & Bladder	100	79.59
Spleen & Bladder	100	81.73
Liver & Bladder	75.27	75.54
Kidney & spleen	76.08	76.52
Liver, spleen & Bladder	78.76	73.23
Kidney, spleen & Bladder	80.00	70.84
Liver, Kidney & Bladder	84.17	75.38
Liver, Kidney & Spleen	88.18	77.72
Liver, Kidney, Bladder & Spleen	73.86	67.92

The overall PCC results based on entropy features are better as compared to energy features. Minimum PCC in two-class classification is obtained for liver and bladder images. This is due to similarity in underlying texture. The result of energy based features for four-class classification is least. The overall performance parameters of spleen



organ images are poor for this experimentation. Table 2 shows these results organ wise.

Organ	Sensitivity	Specificity	Precision	Accuracy
Liver	94.43 %	69.78 %	87.26 %	83.91 %
Bladder	56.34 %	90.21 %	70.99 %	84.40 %
Spleen	33.33 %	91.29 %	26.38 %	85.45 %
Kidney	97.19 %	70.55 %	85.64 %	83.26 %

Table 3 indicates the sample results of second database. This includes the Percentage Correct Classification based on energy features.

Image class	PCC
Liver & Spleen	96.15
Kidney & Bladder	96.66
Spleen & Bladder	97.64
Liver & Bladder	71.11
Liver & Kidney	100
Spleen & kidney	71.03
Liver, Kidney and Spleen	80.42

This algorithm is also tested for noisy images and found to perform well. The PCC for liver and spleen database is 90.38 for both clear and noisy images. The PCC for liver and bladder database is 81.81 and 78.18 for clear and noisy images. PCC for liver, kidney and spleen database is 73.86 and 72.72 for clear and noisy images. This indicates the tolerance of algorithm for the noise in input images. MATLAB 7.1 software has been used for implementation on Pentium IV PC. Image processing and Pattern Recognition toolbox are mainly used.

4.2 Ridgelet based features for normal and abnormal organ images

In liver dataset, 54 normal and 80 abnormal organ images, in brain dataset 77 normal and 62 abnormal images have been used. Liver and brain images are considered for the study of Ridgelet feature performance on healthy and unhealthy organs. Using the same methodology, PCC results and performance measures are derived. PCC results are given in Table 4 and performance measures are given in Table 5.

Classes	PCC
Normal & Abnormal Liver Organ images	84.44 %
Normal & Abnormal Brain Organ images	82.12 %

Organ Images	Sensitivity	Specificity	Precision	Accuracy
Normal Liver	72.20 %	92.59 %	86.67 %	84.40 %
Abnormal Liver	92.59 %	72.20 %	83.33 %	84.40 %
Normal Brain	88.46 %	71.43 %	79.31 %	80.85 %
Abnormal Brain	71.43 %	88.46 %	83.33 %	80.85 %

Discussion

Healthy organs are bearing consistent texture within tissues, across different slices. Hence, the normal organ database is used for this work. In two-class classification subset of PCC result, the least discrimination is between class bladder and liver. This indicates the similarity in two textures.

The precision and sensitivity of spleen is least in this experiment. This indicates that most of the spleen images are misclassified. Specificity of spleen is 91.29%, indicating the other class organs are least misclassified to be spleen. Less precision indicates less exactness in identifying the class as spleen. For other organs sensitivity, specificity and precision are better. This proves the discriminability of features. Accuracy for all the classification results is in the range of 83 to 85%. Sensitivity and precision performance ranges from 33-94% and 26-85% respectively. Spleen organ class is responsible for reducing the values of performance measures. This may be due to less number of spleen images. The database used for this work includes 124 Liver images, 41 Bladder images, 106 Kidney images and 28 Spleen images.

	Liver	Bladder	
Liver	38	4	42
Bladder	8	5	13
	46	9	55

Confusion Matrix 1

A sample Confusion Matrix 1 is computed during liver and bladder two-class classification process. This combination of class gives minimum PCC. It indicates the number of images correctly and incorrectly classified. Out of 42, 38 images are correctly classified as liver and 4 images are misclassified as bladder data. By the ratio of true positives (38) and the total images (42) sensitivity is obtained. Liver sensitivity is 90.48% for this confusion matrix. As 8 images out of 13 of bladder are misclassified as liver, which deteriorates sensitivity of bladder to 38.46%. This is because the underlying textures similarity [27].

	Liver	Kidney	
Liver	42	0	42
Kidney	14	22	36
	56	22	78

Confusion Matrix 2

Confusion Matrix 2 obtained in liver and kidney data classification. This combination of dataset gives better



PCC. All the 42 liver images are correctly classified as liver. This gives 100% sensitivity of liver. 14 kidney images are misclassified as liver, leading to 61.11% sensitivity for kidney. Only sample confusion matrices are represented here for the minimum and maximum PCC values in two-class classification.

For normal and abnormal organ image identification, high specificity is essential. Specificity is 100 % means that all the normal organs are classified as normal. Specificity comments only on one class. To know the performance of other class, sensitivity is determined. It is essential to know the sensitivity of normal class or equivalently specificity of abnormal class. High sensitivity of abnormal class is required for benefit of early diagnosis and treatment as 100 % sensitivity indicates all the results of the class are correct.

5. Conclusions

The comparison of characterization of texture based on energy and entropy feature of Ridgelet transformed images has been carried out. Entropy is the measure of uniformity, which better represents intensity variations. Entropy feature of Ridgelet coefficients is computed to give texture information. Entropy captures the variations of the input information and gives overall better performance than the energy features. Energy features represent the average values in the input. In medical images the randomness of the Ridgelet coefficients better represents a texture. Therefore, results are better for entropy-based features as compared to energy-based features. In two class classification entropy and energy based PCC is 91.89% and 81.82% respectively. Three class classification using entropy and energy based methods give PCC 82.77% and 74.29% respectively and four class classification entropy and energy based PCC is 73.86% and 67.92% respectively.

The size of spleen is small and number of spleen images is less as compared to other images. Therefore, spleen images are mostly misclassified into other dataset, leading to least sensitivity and precision. Overall accuracy and precision of Ridgelet based method is good.

6. Acknowledgements

We acknowledge the help of Department of Radiology and Imaging, Dr. Hedgewar Hospital, Aurangabad, Electronics Department, S.G.G.S.I.E. & T, Nanded during this experiment.

7. References

- [1] J.W.Allison, L.L.Barr, R.J.Masoth, G.P.Berg, B.H.kraner, B.S.Garra, "Understanding the Process of Quantitative Ultrasonic Tissue Characterization", *Radiographics*, Vol.14, pp.1099-1108, 1994
- [2] A.Brubno, R.Collorec, J.B.Wendling, P.Reuze, Y. Rolland, "Texture Analysis in Medical Imaging, Contemporary Perspectives in Three Dimensional Biomedical Imaging", IOS Press, 1997
- [3] J. Duncan, N. Ayache, "Medical Image Analysis: Progress over two decades and the challenges ahead", *IEEE trans on Pattern Analysis and Machine Intelligence*, vol.22, No1, Jan, 2000
- [4] M.Petrou, P.G.Sevilla, "Image Processing Dealing with Texture", John Wiley & Sons, Ltd., 2006
- [5] M. S. Lew, *Principles of Visual Information Retrieval*, Springer, 2001
- [6] J.Koss, F.Newman, T.Johnson, D.Kirch, "Abdominal Organ Segmentation using Texture Transforms and a Hopfield Neural Network", *IEEE trans on Medical Imaging*, vol.18, No.7, Jul 99
- [7] A.Bosnjak, G.Montilla, V.Torrealba, "Medical Images Segmentation using Gabor Filters applied to Echocardiographic Images", *Computers in Cardiology, IEEE*, Vol.25,pp.457-460,1998
- [8] C.Pun & M.Lee, "Log-Polar Wavelet Energy signatures for Rotation and Scale variant Texture Classification", *IEEE trans on Pattern Analysis and Machine Intelligence*, vol.25, No.5, May, 2003
- [9] D.A.Karras, "Improved Defect Detection in Textile Visual Inspection Using Wavelet Analysis and Support Vector Machines", www.icgst.com
- [10] V.Vyas, P.Rege, "Automated Texture Analysis with Gabor Filter", *GVIP Journal*, Vol. 6, Issue 1, July, 2006
- [11] P.S.Hiremath, S.Shivashankar, "Wavelet Based Features For Texture Classification", *GVIP Journal*, Vol. 6, Issue 3, December 2006
- [12] *Handbook on Biomedical Image Analysis*, CRC Press, Chapter 7, pp. 583-638, 2005,LLC
- [13] C.G.Zhao,H.Y.Cheng, Y.L.Huo, T.G.Zhuang, "Liver CT – Image Retrieval Based on Gabor Texture", *Proceedings of 26th Annual international Conference of IEEE, USA*, 1-5, pp. 1491-1494, 2004.
- [14] V.Vyas, P.Rege, "Malignancy Texture Classification in Digital mammograms based on Chebyhev Moments and Logpolar Transformation", *ICGST-BIME Journal*, vol. 7, Issue 1 , December 2007
- [15] M.Do, M.Vetterli, "The finite ridgelet transform for image representation", *IEEE Trans. On Image Processing*, Vol 12., pp16-28, 2003
- [16] N. Malmurugan, A. Shanmugam, S. Jayaraman,A.R. Abdul Rajak, "A Novel Image Compression Algorithm using Ridgelet Transformation with Modified SPIHT", *Academic Open Internet Journal*, ([http:// www.acadjournal.com/](http://www.acadjournal.com/)), Volume 13, 2004
- [17] J.L.Starck, E.J.Candès, D.L.Donoho, "The Curvelet Transform for Image Denoising", *IEEE Trans. On Image Processing*, Vol. 11, No.6, pp.670-684, June, 2002
- [18] A.G. Flesia, H. Hel-Or, A. Averbuch, E.J. Cand'es, R.R. Coifman, D.L. Donoho J. Stoeckler and G. V. Welland, "Digital



Implementation of Ridgelet Packets”, Academic Press, Inc, 2001

- [19] A.K.Jain, Fundamentals of Digital Image Processing, PHI, July, 2001
- [20] D.Chaudhari, “IP for target detection Classification”, STTP on Image Processing Applications, June, 2003
- [21] D.G.Stork, E.Y.Tov, Computer Manual in MATLAB to accompany Pattern Classification, II Edition, Wiley Interscience, John Wiley & Sons INC, Publication, 2004
- [22] R.P.W.Duin, PRTools version 3.0A Matlab toolbox for Pattern Recognition, Jan. (<http://www.ph.tn.tudelft.nl/prtools>), 2000
- [23] R.O.Duda, P.E.Hart, D.G.Stork, “Pattern Classification”, II Edition, Wiley Interscience, John Wiley & Sons INC, Publication, 2001
- [24] R.C.Gonzalez, R.E.Woods, S.L.Eddins, Digital Image Processing Using MATLAB, Pearson Education, 2004
- [25] J.Kovacevic,A.Chebira, “Life Beyond Bases : The Advent of Frames Part I”, IEEE Signal Processing Magazine, pp 86-104, July, 2007
- [26] Image Processing Toolbox, For use with MATLAB, The Maths Work Inc, 2001
- [27] R.J.Schalkoff, Pattern Recognition: Statistical, Structural and Neural Approaches, John Wiley & Sons Inc, 1992

Biographies



V.R.Ratnaparkhe is working on “Biomedical Image Analysis” for the research project. She received M.Tech degree from C.E.D.T. in 1996. She is working as lecturer in Electronics Department, Government Polytechnic of Maharashtra State at Aurangabad, India. Her area of interest is Image Processing and Pattern Recognition
patwadkar.varsha@gmail.com



R.R. Manthalkar received his B.E (1988) and M.E. (Electronics) (1994) from SGGS Institute of Engg & Technology, Nanded, India. He was Rank I for BE(Electronics) in the University. He completed Ph.D. from IIT Kharagpur (2003). He has published many research papers in Journals (7) and Conferences (20). His research interests are Texture Classification and Pattern Recognition. Currently he is Assistant Professor in SGGS Institute of Engg & Technology, Nanded, M.S., India
rmanthalkar@yahoo.com



Y.V. Joshi received his B.E. (1986) and M.E. (Electronics) (1994) from SGGS Institute of Engg & Technology, Nanded, India.. He completed Ph.D. from IIT Delhi (2003) . His research interests are VLSI, Signal & Image Processing. He has published seven research papers in Journals and more than 20 papers in Conferences. Currently he is Professor in SGGS Institute of Engg & Technology, Nanded, and M.S., INDIA.
yashwant.joshi@gmail.com

